Unstable nuclei in dissociation of light stable and radioactive nuclei in nuclear track emulsion

D. A. Artemenkov and P. I. Zarubin

V. I. Veksler and A. M. Baldin Laboratory of High Energy Physics,
Joint Institute for Nuclear Research, Dubna, Russia

Abstract. Recent results of nuclear clustering studies obtained by means of the nuclear track emulsion (NTE) technique are reviewed with a special impact on the role of the unstable ^{8}Be and ^{9}B nuclei.

Exposure of NTE to nuclei ^{8}He of energy of 60 MeV made it possible to identify decays of stopped ^{8}He nuclei, estimate possibilities of α-range spectrometry and observe the drift of thermalized ^{8}He atoms. Correlations of α-particles studied in splittings ^{12}C → 3α induced by 14.1 MeV neutrons indicate the presence of a superposition of the 0^+ and 2^+ states of the nucleus ^{8}Be in the ground state of ^{12}C. The study in boron enriched NTE of the angular correlations of fragments produced by thermal neutrons is pointed to production of the exited ^{7}Li nucleus.

Contribution of the unstable nuclei ^{6}Be, ^{8}Be and ^{9}B to the dissociation of relativistic nuclei ^{7,9}Be, ^{10}B and ^{10,11}C is under study on the basis of NTE exposed to secondary beams of the JINR Nuclotron. Contribution of the configuration ^{6}Be + n to the ^{7}Be structure is estimated at a level of 8 ± 1 % which is near the value for the configuration ^{6}Li + p. Distributions over the opening angle of α-pairs indicate to a simultaneous presence of virtual ^{8}Be$_{g.s.}$ and ^{8}Be$_{2+}$ states in the ground states of the ^{9}Be and ^{10}C nuclei. The core ^{9}B is manifested in the ^{10}C nucleus with a probability of 30 ± 4 %. ^{8}Be$_{g.s.}$ decays are presented in 24 ± 7 % of 2He + 2H and 27 ± 11 % of the 3He of the ^{11}C "white" stars. ^{9}B decays are identified in "white" stars ^{11}C → 2He + 2H constituting 14% of the ^{11}C "white" stars. As in the ^{10}C case the ^{8}Be$_{g.s.}$ decays in ^{11}C "white" stars almost always arise through ^{9}B decays. On this ground the channel ^{9}B + H amounts 14 ± 3 %. The ^{8}B$_{g.s.}$ nucleus is manifested in the "white" stars ^{10}B → 2He + H with a probability of 34 ± 7 % while ^{9}B constitute 14 ± 4 %.

Introduction

Highlights of nuclear clustering in light nuclei studies obtained recently by means of the nuclear track emulsion technique (NTE) in the framework of the BECQUEREL Project [1] are gathered here. As fundamental "building blocks" the light nuclei include the lightest clusters having no excited states, namely, α-particles, tritons, ^{3}He nuclei, and deuterons, and nucleons which virtual associations coexist in dynamical equilibrium. The family of nuclei composing the beginning of the isotope table provides a wholesome "laboratory" which allows one to study the evolution from cluster to shell nuclear structure (fig. 1). A pair of α-particles can constitute an unstable ^{8}Be nucleus in the ground ^{8}Be$_{g.s.}$ or 1st exited ^{8}Be$_{2+}$ states. The stable ^{7}Be and ^{7}Li nuclei are important in the structure of the neutron deficient and neutron rich nuclei, respectively. When the nucleons or clusters are added to the ^{8}Be, ^{7}Be and ^{7}Li nuclei the last ones serve as cores in the subsequent stable and radioactive isotopes. Then, the unstable ^{9}B and stable ^{9}Be can play a core role of an equal importance in heavier nuclear structures. A balanced superposition of the cores, clusters and nucleons in appropriate spin-parity states determine ground state parameters of a corresponding nucleus.
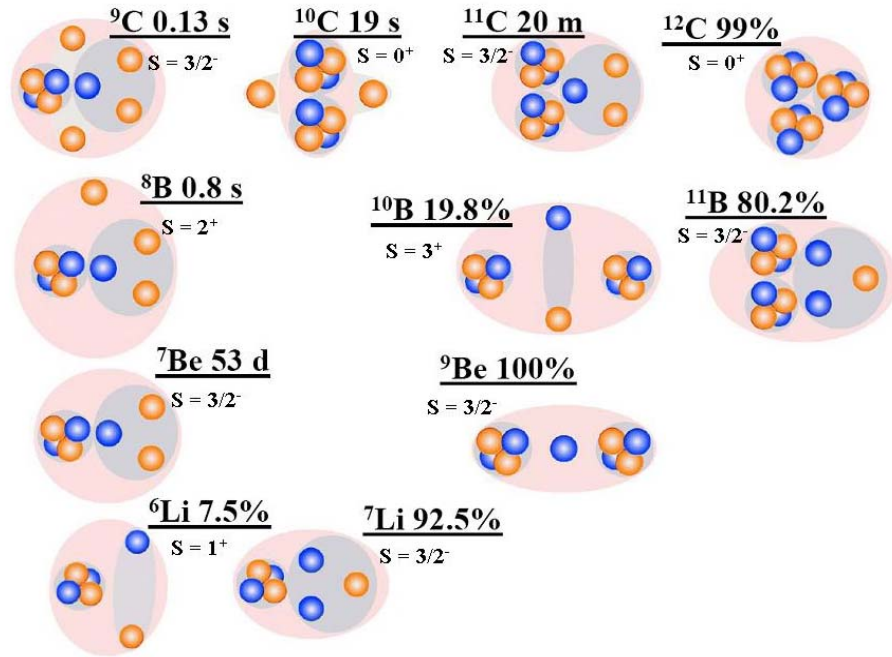
Fig. 1. (Color online). Diagram of cluster degrees of freedom in stable and neutron-deficient nuclei; abundances or lifetimes of isotopes, their spins and parities are indicated; open circles correspond to protons and dark ones − neutrons; clusters are marked as dark background.

In spite of the fact that half a century passed since the NTE development it retains the status of an universal and inexpensive detector [2-4]. With an unsurpassed spatial resolution (about 0.5 μm) NTE of the BR-2 type provides a complete observation of tracks starting from fission fragments and down to relativistic particles. NTE deserve a further use in fundamental and applied research in state-of-art accelerators and reactors, as well as with sources of radioactivity, including natural ones. Application of NTE is especially justified in those pioneering experiments in which nuclear particle tracks can not be reconstructed with the help of electronic detectors. Thus, in the last decade in the framework of the BECQUEREL Project in JINR the NTE technique allowed one to investigate clustering of the nuclei ^{7}Li, ^{7,9}Be, ^{8,10}B, ^{9,10}C and ^{12,14}N in their relativistic dissociation [4-12].

However, the production of NTE pellicles which lasted in Moscow for four decades was ended more than ten years ago. The interest in a further application stimulated its reproduction in the MICRON workshop that is part of the company "Slavich" (Pereslavl Zalessky) [13]. At present NTE samples are produced by layers of thickness of 50 to 200 μm on glass substrates. Supportless pellicles of thickness of the order of 500 μm are expected to be available soon. Verification of novel NTE in exposures to relativistic particles confirmed that it is similar to the BR-2 one.

The NTE technique is based on intelligence, vision and performance of researchers using traditional microscopes. Despite widespread interest, its labor consumption causes limited samplings of hundreds of measured tracks which present as a rule only tiny fractions of the available statistics. Implementation of computerized and fully automated microscopes in the NTE analysis allows one to bridge this gap. These are complicated and expensive devices of collective or even remote usage allow one to describe unprecedented statistics of short nuclear tracks. To make such a development purposeful it is necessary to focus on such a topical issue of nuclear physics the solution of which can be reduced to simple tasks of recognition and measurement of tracks in NTE to be solved with the aid of already developed programs.

Keeping in mind such a perspectve competitiveness of NTE in measurements of short α-particle and heavy ion tracks on the most precise optical microscope KSM with a 90× objective

is demonstrated in series of low energy applications. When measuring decays of ^{8}He nuclei implanted in NTE the possibilities of α-spectrometry were verified and the effect of the ^{8}He atom drift was established [14-16]. Correlation of α-particle triples were studied in disintegrations of carbon nuclei of NTE composition by 14.1 MeV neutrons [17]. The angular correlations of ^{7}Li and ^{4}He nuclei produced in disintegrations of boron nuclei by thermal neutrons were studied in boron enriched NTE [18]. In this series of exposures the angular resolution of NTE was confirmed to be perfect by expected physical effects which are manifested in the distributions of the opening angles distributions of the products of the studied reactions.

At CERN, a NTE sample was exposed to 160 GeV muons [18]. The irradiation of track emulsions with these particles makes it possible to study concurrently the multifragmentation of nuclei under the effect of a purely electromagnetic probe. Multiphoton exchanges or transitions of virtual photons to vector mesons may serve as a fragmentation mechanism. The nuclear diffraction mechanism rather than the soft electromagnetic mechanism manifests itself for the channel of carbon nuclei splittings to α-particle triples. The corroboration of this conclusion is of importance for interpreting not only multifragmentation under the effect of ultrarelativistic muons. It may also serve as a basis for interpreting the multifragmentation of relativistic nuclei in peripheral interactions not leading to the formation of target fragments ("white" stars)

One of the suggested problems is a search for the possibility of a collinear cluster tri-partition [19]. The existence of this phenomenon could be established in observations of such a type of ternary fission of heavy nuclei in which a lightest fragment is emitted in the direction of one of the heavy fragments. Despite distinct observability of fission fragments they can not be fully identified in NTE. However, NTE is valuable due to the combination of the best angular resolution and maximum sensitivity. Besides, it is possible to measure the lengths and thicknesses of tracks, and, thus, to classify the fragments. As an initial stage, to provide statistics of ternary fissions it is suggested to analyze a sufficient NTE area exposed to ^{252}Cf source with an appropriate density of tracks of α-particles and spontaneous fission fragments [20]. Such an approach will be developed by a NTE with an admixture of the ^{252}Cf isotope [5,6]. Another option is exposure of NTE manufactured with a ^{235}U isotope addition by thermal neutrons.

On high energy side novel NTE was exposed quite recently to the secondary beam of relativistic nuclei ^{11}C of the JINR Nuclotron which allowed one to include a clustering of the ^{11}C nucleus into the general pattern already relying on data on the light nuclei including radioactive ones. The ^{11}C data stimulated an additional analysis of previous ^{10}C and ^{10}B exposures.

Low energy exposures
Stopped ^{8}He nuclei
Exposure of NTE to nuclei ^{8}He of energy of 60 MeV [4] is performed at the fragment separator ACCULINNA in the G. N. Flerov Laboratory of Nuclear Reactions, JINR. Features of decays of the ^{8}He isotope are shown in Fig. 2, according to the compilation [21]. Fig.4 shows macrophotographs of decays of ^{8}He nuclei stopped in NTE. They are typical ones among thousands observed in this study. Videorecordings of such decays taken with the microscope and camera are collected [1].

A search for β-decays of ^{8}He nuclei was focused on hammer-like events (Fig. 3). Often, in the events named "broken" ones gaps were observed between stopping points of primary tracks and subsequent hammer-like decays. The "broken" events were attributed to a drift of thermalized ^{8}He atoms that arose as a result of neutralization of ^{8}He nuclei. Arrival directions and stopping points of ions ^{8}He, their decay vertices and stops of decay α-particles were determined for 136 "whole" and 142 "broken" events. In "broken" events the decay points were determined by extrapolating the electron tracks. The distribution of the opening angles of α-particle pairs has a mean value 164.9±0.7°. The kinks of "hammers" are defined by the momenta carried away by ev-pairs.
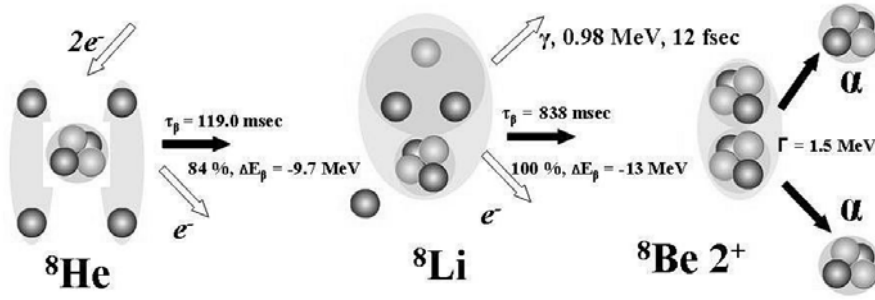
Fig. 2. Scheme of a major channel of the cascade decay of ^{8}He isotope; light circles correspond to protons, dark ones neutrons

The dependence of the α-particle ranges and their energy values are determined by spline interpolation of calculations in the SRIM model [22]. Knowledge of the energy and emission angles of α-particles allows one to derive the energy distribution of α-decays $Q_{2\alpha}$. The invariant variable Q is defined as the difference between the invariant mass of a final system M^* and the mass of a primary nucleus M. M^* is defined as the sum of all products of the 4-momenta P_i of fragments, that is, $M^{*2} = (\sum P_i)^2$. In general, the distribution of $Q_{2\alpha}$ (Fig. 4) corresponds to the ^{8}Be$_{2+}$ decay. However, the mean value of $Q_{2\alpha}$ is slightly higher than expected. This fact is determined by the presence of a "tail" of large values $Q_{2\alpha}$, obviously not matched by a Gauss fit. For events with both α-particle ranges above 12.5 μm and opening angles above 145° a mean value of $Q_{2\alpha}$ equal to 2.9 ± 0.1 MeV at RMS 0.85 MeV, which corresponds to the ^{8}Be$_{2+}$ state. The insertion in Fig. 4 shows $Q_{2\alpha}$ for additional statistics corresponding to both ranges above 12.5 μm. The physical reason for the appearance of the "tail" in the distribution $Q_{2\alpha}$ is not clear. Probably, its shape reflects spatial structure the ^{8}Be$_{2+}$ state.

In the "broken" events the distances $L(^8$He–^{8}Be) between the stopping points of the ^{8}He ions and the decay vertices as well as the angles $\Theta(^8$He–^{8}Be) between arrivaldirections of the ions and directions from the stopping points of the ions towards the decay vertices are defined (Fig. 5). Uniformity of distributions of events over these parameters and the absence of a clear correlation indicate on a thermal drift of the atoms ^{8}He. The mean value of $L(^8$He–^{8}Be) amounting to 5.8 ± 0.3 μm at rms 3.1 ± 0.2 μm, can be associated with a mean range of atoms ^{8}He. The low value of a mean speed of the atoms ^{8}He defined as ratio of the mean value of $L(^8$He–^{8}Be) to the half-life of the nucleus ^{8}He supports a pattern of diffusion.

As a next step, it appears to be interesting to study angular ββ correlations in order to search for conservation of polarization of intermediate ^{8}Li nuclei. In perspective, observation of the diffusion points to the possibility of generating of radioactive atoms ^{8}He and pumping them out of sufficiently thin targets. Increasing of the mean speed and drift length is achievable due to heating of the target. In this way, there is a prospect of accumulating of a significant amount of ^{8}He atoms. Besides, an applied interest consists in studies of thin films by pumping atoms ^{8}He and their deposition on α-detectors.

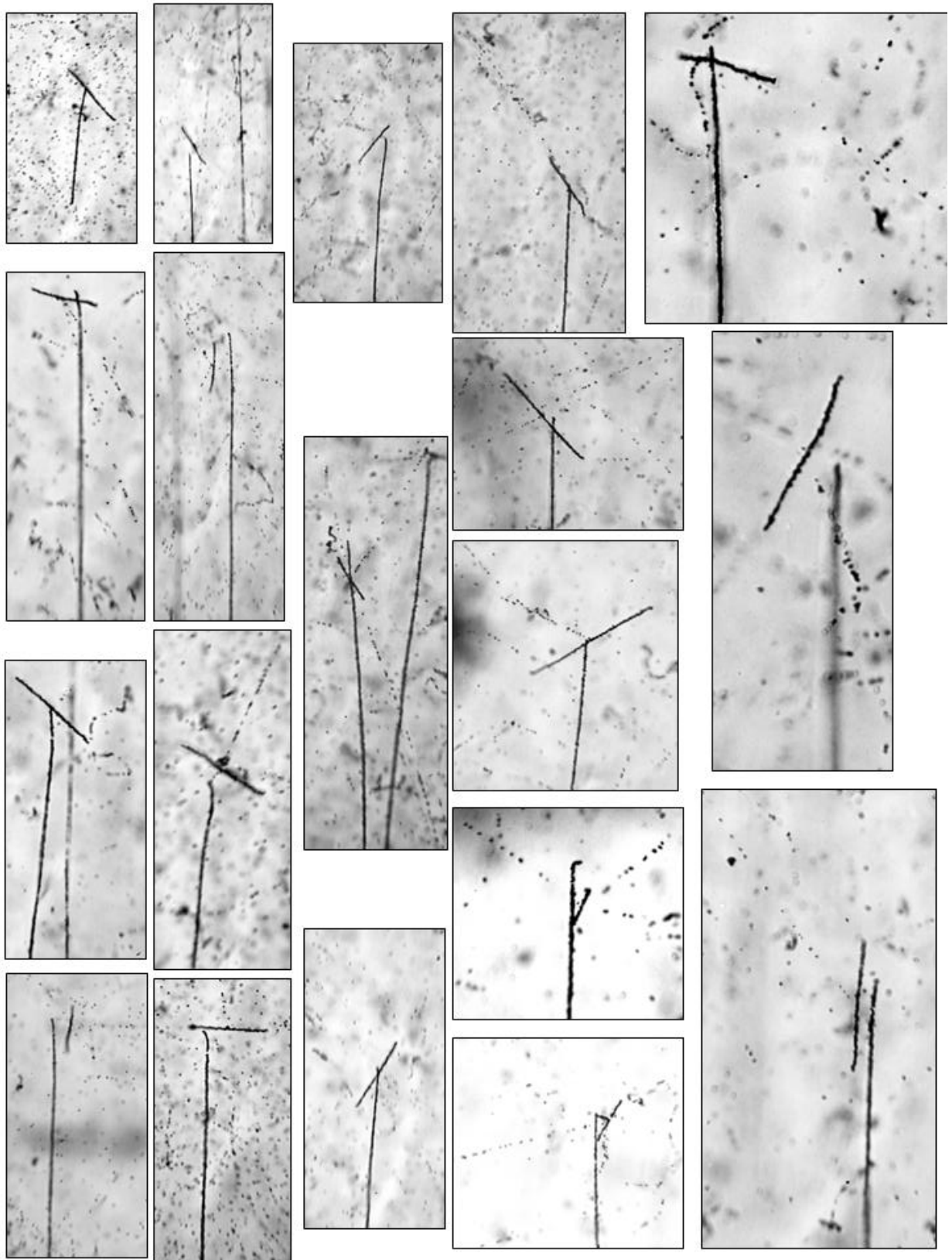Fig. 3. Macrophotographs of hammer-like decays of ^{8}He nuclei stopped in NTE; started from bottom ^{8}He tracks are oriented vertically; short tracks correspond to $^8Be_{2+}$ decay; dotted tracks produced by decay electrons.

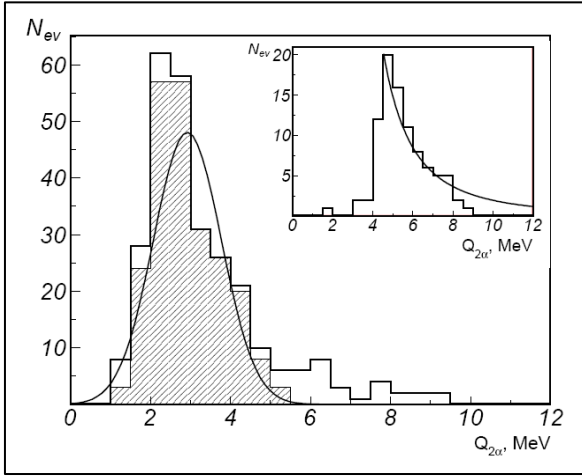Fig. 4. Distribution over energy $Q_{2\alpha}$ of 278 pairs of α-particles; hatched histogram corresponds to events with α-particle ranges less than 12.5μm; line is Gaussian fit. Insertion: $Q_{2\alpha}$ distribution of additional 98 pairs with α- particle ranges above 12.5 μm.
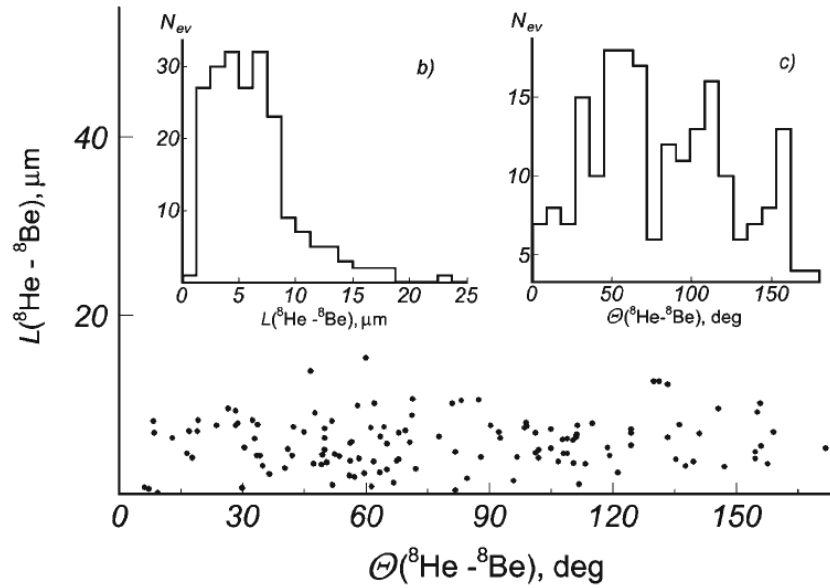

Fig. 5. Distribution of distances L(^{8}He–^{8}Be) between stopping points of ^{8}He ions and their decay vertices over rangles Θ(^{8}He–^{8}Be) between directions of arrivals of the ions and directions from stopping points of the ions to decay vertices; Insertions: projections L(^{8}He–^{8}Be) (b) and Θ (^{8}He–^{8}Be) (c).

3α-particles splitting of ^{12}C nuclei by neutrons

The ^{12}C nucleus is a recognized departure point for the development of α-particle clustering concepts. It is possible that the ground state ^{12}C$_{g.s.}$ contains two bounds of α-clusters with each one possessing an orbital angular moment of two units (D-wave) corresponding to the 1st excited state ^{8}Be$_{2+}$. A rotation in opposite directions of two α-clusters with angular momenta equal to 2 around a common center represented by a third α-cluster can be imagined corresponding to the ground state ^{8}Be$_{g.s.}$ (S-wave). As a result the superposition of the ternary pairing leads to a zero spin of ^{12}C$_{g.s.}$. This simplified pattern can manifest itself in an intensive or even simultaneous production of the unstable ensembles ^{8}Be$_{2+}$ and ^{8}Be$_{g.s.}$ in ^{12}C break-ups.

Such a concept does not contradict to the accepted scenario of the ^{12}C synthesis (fig. 6). Fusion of an α-particle triple with starts when the triple turns out in the ^{12}C 2nd excited state 0^+_2 (the Hoyle state). This state located on 270 keV above the breakup threshold ^{12}C $\rightarrow$ 3α can be considered as triple superposition ^{8}Be$_{g.s.}$ since each α-particle pair is 90 keV above binding like ^{8}Be$_{g.s.}$. Transition to the ^{12}C 1st excited state which is bound one occurs when a photon carrying away 2 units of spin is emitted out of the triple ($0^+_2 \rightarrow 2^+_1$). This way a D-wave α-pair arises in

6

the triple due to angular momentum conservation. A subsequent transition to the ground state $^{12}C_{g.s.}$, which is also accompanied by emission of a photon leads to formation of another D-wave α-particle pair. This pair should have an opposite angular momentum with respect to the first one to ensure zero spin value of the ground state $^{12}C_{g.s.}$. Thus, the ^{12}C nucleus does acquire a hidden polarization. Figuratively being expressed it does conserve an "invisible rotation".

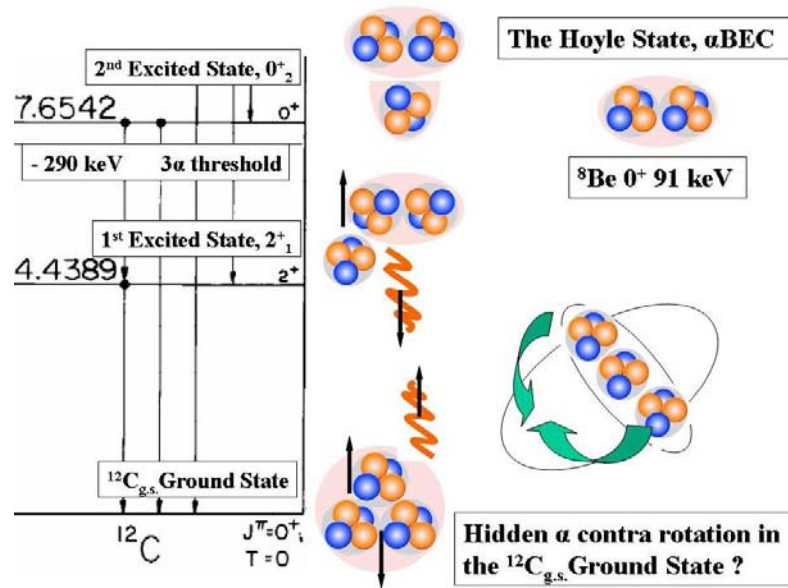Fig. 6. Diagrams of ^{12}C synthesis via 3α process.

The yield of α-particle pairs through the states $^{8}Be_{2+}$ and $^{8}Be_{g.s.}$ not accompanied by a transfer of the angular momentum can reflect such a spin-cluster structure of the $^{12}C_{g.s.}$ state. Study of α-particle triples is possible in disintegrations of carbon nuclei of NTE composition by neutrons of energy of 14.1 MeV. Energy transferred to α-particles is sufficient to measure their ranges and directions and, at the same time, it remains below the thresholds of background channels. The stack of NTE layers is exposed to neutrons produced in the reaction $d + t \rightarrow n + \alpha$ on one of devices DVIN of an applied destination [23]. Scanning of the layers was aimed at 3α-disintegrations. In 400 events of 3α-disintegration selected among the found 1200 ones measurements of angles relative to plane of a NTE layer and its surface as well as their lengths were at a KSM microscope performed for all α-particle tracks. The only condition for the selection of the events was fullness of measure.
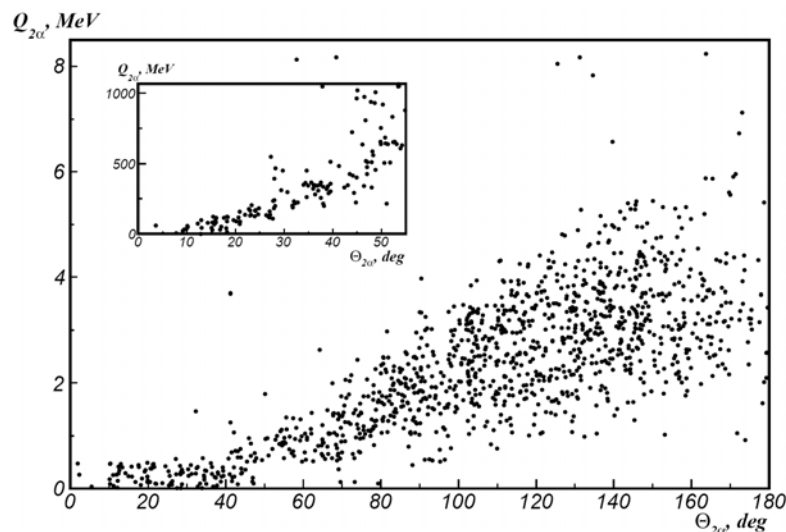

Fig. 7. Correlation over energy $Q_{2\alpha}$ and opening angles $\Theta_{2\alpha}$ in α-particle pairs

Determination of angles and energy values versus ranges in the SRIM model allowed one to determine the energy $Q_{2\alpha}$ of pairs. Correlation over energy $Q_{2\alpha}$ and opening angles $\Theta_{2\alpha}$ in α-particle pairs indicate on ^{8}Be features (Fig. 7). The region of large opening angles $\Theta_{2\alpha} > 90^o$ corresponds to $Q_{2\alpha}$ of ^{8}Be$_{2+}$, while $\Theta_{2\alpha} < 40^o$ - ^{8}Be$_{g.s.}$. The distribution over $Q_{2\alpha}$ points to both states (Fig. 8) but rather smeared due to the cluster knock outs by neutrons. Rough condition $Q_{2\alpha} < 500$ keV allows to allocate about 110 decays ^{8}Be$_{g.s.}$. The ^{8}Be$_{g.s.}$ selection leads to simultaneous appearance of a second peak with the mean value $Q_{2\alpha}$ equal to 2.52 ± 0.04 MeV at rms 1.2 MeV corresponding to the ^{8}Be$_{2+}$. Thus, despite to complicated mechanism of the few-body reaction ^{12}C(n,n')3α an coexistence of the virtual nuclei ^{8}Be$_{2+}$ + ^{8}Be$_{2+}$ + ^{8}Be$_{g.s.}$ in the ^{12}C ground state appears to be manifested in a least of a quarter of 3α-disintegrations.
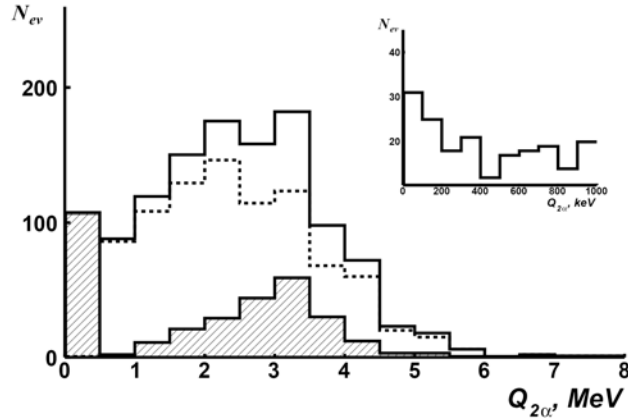

Fig. 8. Distribution α-particle pairs produced in ^{12}C disintegrations by 14 MeV neutrons over energy $Q_{2\alpha}$ of (solid), α-pairs with selection of ^{8}Be$_{g.s.}$ (hatched) and their difference (dashed).

Importance of the discussed structure is determined not only by the interest to describe ^{12}C$_{g.s.}$, but also the fact that it is the starting configuration for a reverse process of generating 3α-particle ensembles in the Hoyle state. It is assumed that this state after ^{8}Be$_{g.s.}$ is a Bose-Einstein condensate consisting of α-particles with zero angular momentum [9]. Its identification in breakups of ^{12}C allows one to advance to generation of condensate states of a larger number of α-particles. A fundamental aspect appears to be related to the fact that to recreate the condensate it is necessary to "evacuate" two hidden rotation ^{12}C$_{g.s.}$. In this respect the Coulomb dissociation of a nucleus on a heavy nucleus appears to be the most suitable process since multiple exchanges photons are possible in it.

Thermal neutron exposure
Samples of NTE prepared with the addition of boric acid were trasversily exposed 30 min to a thermal neutron beam of the JINR IBR-2 reactor. Enrichment of NTE with boron allows one to observe charged products of the reaction $n_{th} + {}^{10}$B $\rightarrow {}^7$Li + (γ) + ^{4}He. This reaction giving output of energy of 2.8 MeV occurs with a probability of about 93% with the emission of γ-ray of energy of 478 keV by the nucleus ^{7}Li in a single excited state. Coordinate measurements of tracks of 112 events ^{7}Li + ^{4}He are performed. Directions of emission are not collinear in pairs as a consequence of γ-emission. The average opening angle $\Theta(^7$Li + ^{4}He) is 148 ± 14°. The average value of Q(^{7}Li + ^{4}He) amounted to 2.4 ± 0.2 MeV (RMS 0.8 MeV) correspond tothe expected one when taking into account the energy carried away by γ-quanta. The distribution $\Theta(\gamma + {}^7$Li) of angles between the directions of emission of γ-quanta computed according to the condition of conservation of momentum and the directions of emission of the nuclei ^{7}Li shows a clear anticorrelation (Fig. 9).
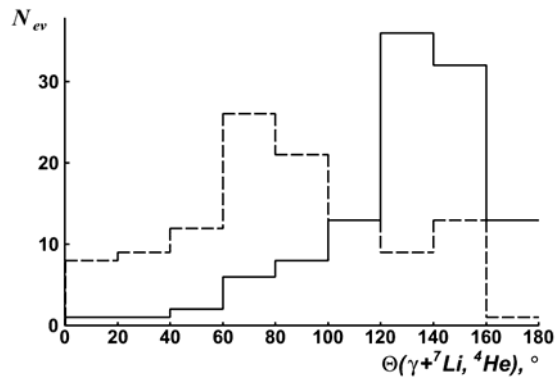
Fig. 9. Distribution over the angle $\Theta(\gamma + {}^7\text{Li}, {}^4\text{He})$ between the calculated directions of emission of γ-quanta and the directions of emission of nuclei ${}^7\text{Li}$ (solid) and ${}^4\text{He}$ (dashed) produced by thermal neutrons in 112 events $n_{\text{th}} + {}^{10}\text{B} \to {}^7\text{Li} + (\gamma) + {}^4\text{He}$.
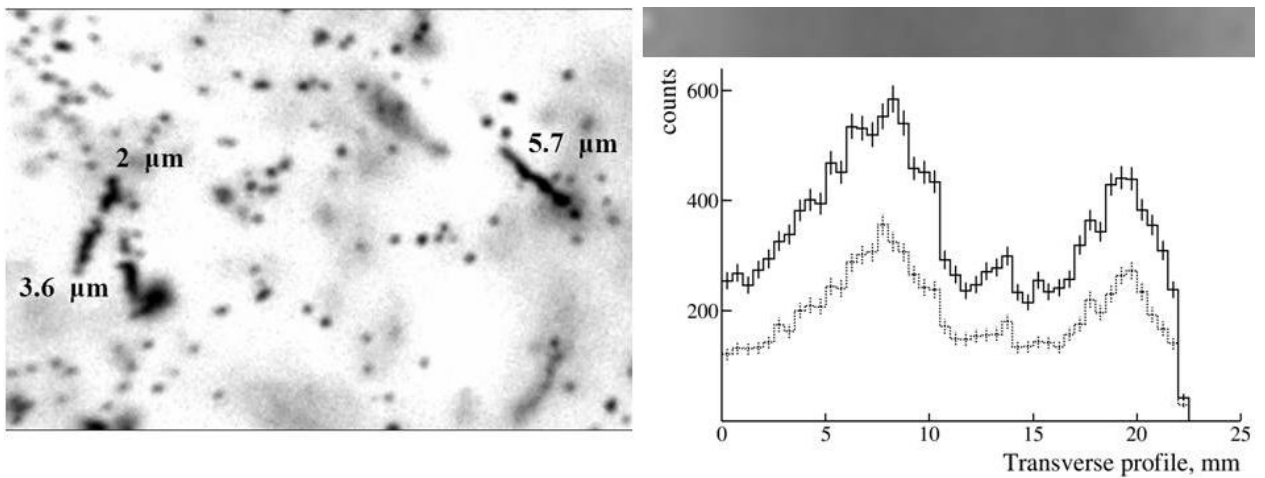

Fig. 10. Macrophotograph of typical tracks in boron enriched NTE (left); a scanned strip of a length 25 mm (right top); distribution of Li + He (up) and alone He (down) tracks along transverse direction of neutron beam spot in NTE.

The experience of a computer analysis of tracks produced by thermal neutrons in boron enriched NTE is obtained using the microscope HSP-1000 of the Department of Radiation Dosimetry of Nuclear Physics Institute in Prague. Recognition Li + He and alone He tracks by the ImageJ program [24] performed along allowed one to find up to 16000 events along a scanned 25 mm strip and a width of a 1 mm and on this basis restore the transverse profile of the thermal neutron beam (fig. 10).

High energy exposures
Nuclear clustering in relativistic dissociation

Consideration of the nucleosynthesis chains toward ${}^{10,11}\text{B}$, ${}^{11,10}\text{C}$ and ${}^{12}\text{N}$ via the "hot breakout" ${}^7\text{Be}({}^3\text{He},\gamma){}^{10}\text{C}(e^+,v){}^{10}\text{B}$ assists to recognize the interconnections in their structures and, in particular, importance of the unbound nuclei in them. The ${}^{10}\text{C}$ synthesis processing due to an increase of α-clustering provides an energy "window" for the formation of intermediate states with unstable nuclei ${}^9\text{B} + p$, ${}^8\text{Be}_{2+} + 2p$ and ${}^6\text{Be} + \alpha$. These clusters are preserved in subsequent reactions ${}^{10}\text{C}(e^+,v){}^{10}\text{B}(p,\gamma){}^{11}\text{C}(e^+,v){}^{11}\text{B}$. The "window" of the reaction ${}^7\text{Be}({}^4\text{He},\gamma){}^{11}\text{C}$ allows only an association of the ${}^7\text{Be}$ and ${}^4\text{He}$ clusters, also contributing to the ${}^{11}\text{C}$ and ${}^{10}\text{B}$ structure. Thus, a hidden variety of the virtual configurations in the nuclei ${}^{10,11}\text{C}$ and ${}^{10,11}\text{B}$ can be populated via electromagnetic transitions from the real ones. In turn, these nuclei provide a basis for capture reactions of protons or the He isotopes (or in neutron exchange) for synthesis of the subsequent

nuclei which leads to a translation of the preceding structures. Obviously, the unstable nuclei ^{8}Be and ^{9}B play a key role in a general pattern of nuclear clustering and despite complicated observability their contribution deserves to be studied in detail over an available variety of light nuclei and physical mechanisms.
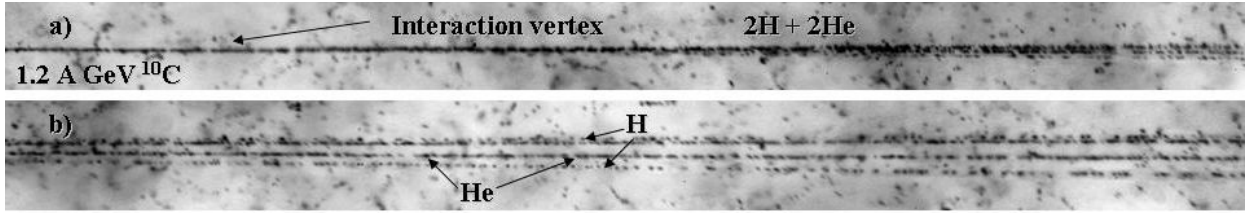

Fig. 11. Macrophoto of the coherent dissociation event of 1.2 A GeV ^{10}C nucleus into pairs of He and H nuclei; a) primary track, approximate position of interaction vertex and appearance of fragment tracks and b) tracks of fragments are resolved; opening angles between tracks are Θ_{2He} = 5.9 mrad, Θ_{HeH} = 8.6, 16.6, 3.0, 17.6 mrad, Θ_{2p} = 20.1 mrad. Both 2HeH triples in the event correspond to ^{9}B decays.

The cluster structure of light nuclei including radioactive ones in relativistic-fragmentation processes is a central topic of the BECQUEREL project which continue the tradition of use of the NTE technique [5]. Such reactions are under study by means of NTE stacks longwise exposed to primary and secondary beams of relativistic nuclei of the JINR Nuclotron. Among the events of fragmentation of relativistic nuclei, those of their coherent dissociation to narrow jets of fragments are especially valuable for studying nuclear clustering. Coherent dissociation does not feature either slow fragments of NTE composing nuclei or charged mesons. This empirical feature allows one to assume a glancing character of such collisions and that excitations of relativistic nuclei under study are minimal. A main underlying mechanism of coherent dissociation is nuclear diffraction interaction processing without nuclear density overlap and angular momentum transfer. The experimental method in question has already furnished unique information compiled in [5] about cluster aspects of the structure of the whole family of light nuclei, including radioactive ones.

Events of coherent dissociation are called "white" stars because of the absence of tracks of strongly ionizing particles (fig. 11). The term "white" star reflects aptly a sharp "breakdown" of the ionization density at the interaction vertex upon going over from the primary-nucleus track to secondary tracks within a 6^0 cone at 1.2 A GeV. This special feature generates a fundamental problem for electronic methods because more difficulties should be overcome in detecting events where the degree of dissociation is higher. On the contrary, such events in NTE are observed and interpreted in the most straightforward way, and their distribution among interaction channels characterized by different compositions of charged fragments is determined exhaustively.

The probability distribution of the final configurations of fragments in "white" stars makes it possible to reveal their contributions to the structure of nuclei under consideration. We assumed that, in the case of dissociation, specific configurations arise at random without sampling and that the dissociation mechanism itself does not lead to the sampling of such states via angular-momentum or isospin exchange. By and large, available results confirm the assumption that the cluster features of light nuclei determine the pattern of their relativistic dissociation. At the same time, events that involve the dissociation of deeply bound cluster states and which cannot arise at low collision energy are detected.

Data on the previously studied nuclei are valuable ingredients of the ongoing analysis, and deserve a brief description. The feature of ^{7}Be dissociation is an approximate equality of probability of the main channels 2He and He + 2H of coherent dissociation (table 1). Their ratio is equal to 0.7 ± 0.1 [11]. The channel 2He + H leads among ^{10}B "white" stars reaching about 75% (Table. 2). Events of channel He + 3H are 12%. 10% of the events contain both fragments Li and He. Only 2% of the events contain fragments Be and H indicating a minor probability of

configuration ^{9}Be + p in the ^{10}B structure. In contrast, the contribution of the channel ^{7}Be + p in the ^{8}B coherent dissociation is a leading one while the configurations containing only clusters of He and H are estimated at 50%.

Table 1. Distribution ^{7}Be "white" stars produced over charge channels.

channel	^{7}Be [8]
2He	115 (40 %)
He + 2H	157 (54 %)
Li + H	14 (5 %)
4H	3 (1 %)

Table 2. Distribution ^{10}B and ^{8}B "white" stars over charge channels.

channel	^{10}B	^{8}B
Be + H	1 (2 %)	25 (48 %)
2He + H	30 (73 %)	14 (27 %)
He + 3H	5 (12 %)	12 (23 %)
Li + He	5 (13 %)	

The unstable nuclei in dissociation of the ^{9}Be, ^{10}C and ^{7}Be nuclei

Reconstruction of the decays of relativistic ^{8}Be and ^{9}B nuclei is possible by the energy variable $Q = M^* - M$, where $M^{*2} = \sum(P_i \cdot P_k)$, M is the total mass of fragments, and $P_{i,k}$ are their 4-momenta defined under the assumption of conservation of an initial momentum per nucleon by fragments. When the identification of relativistic fragment can be reasonably supposed the quasi-invariant variable Q allows one to estimate the excitation energy of their complex ensembles uniting all angular measurements in an event. For the "white" stars of ^{9}Be and ^{10}C nuclei the assumption that He fragments correspond to ^{4}He nuclei (α), and H ones in ^{10}C – ^{1}H (p) is justified. Then ^{8}Be and ^{9}B identification is reduced to measurements of the opening angles between the directions of fragment emission. The experimental details and development of these investigations and their illustrations are presented in [5].

Distributions over the opening angle Θ_{2He} for pairs of He fragments of "white" stars ^{9}Be $\to$ 2He and ^{10}C $\to$ 2He + 2H (82% of the ^{10}C statistics) produced at energy of 1.2 A GeV are presented in Fig. 12. In both cases the values of Θ_{2He} of 75-80% of the pairs are distributed about equally in the intervals of $0 < \Theta_{n(arrow)} < 10.5$ mrad and $15.0 < \Theta_{w(ide)} < 45.0$ mrad. The remaining pairs are attributed to intervals $10.5 < \Theta_{m(edium)} < 15.0$ and "widest" of $15.0 < \Theta_{v(ery)w(ide)} < 45.0$ mrad. The distribution over the Q variable is directly correlated with the Θ_{2He} one. It is pointing out that "narrow" pairs of Θ_n are produced via ^{8}Be$_{g.s.}$ while pairs Θ_w via ^{8}Be$_{2+}$. Besides, for the ^{9}Be case there is a peak in the interval Θ_m reflecting its level 5/2$^-$ (2.43 MeV). Fractions of events in the intervals Θ_n and Θ_w are equal to 0.56 ± 0.04 and 0.44 ± 0.04 for ^{9}Be, while for ^{10}C 0.49 ± 0.06 and 0.51 ± 0.06, i. e. they practically coincide. They indicate to a simultaneous presence of virtual ^{8}Be$_{g.s.}$ and ^{8}Be$_{2+}$ states in the ground states of the ^{9}Be and ^{10}C nuclei. Elongation above 40 mrad of the ^{10}C Θ_{2He} distribution can be due to the channel ^{4}He + ^{6}Be.
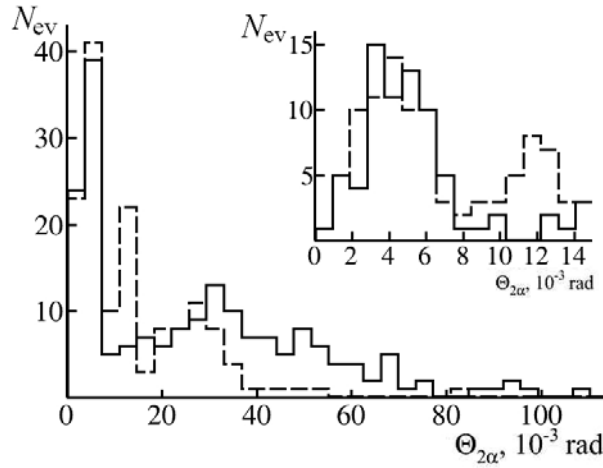
Fig. 12. Distributions over the opening angle Θ_{2He} of α-particle pairs in "white" stars ^{10}C → 2He + 2H (solid) and ^{9}Be → 2He (dashed); on the insertions: the Θ_{2He} distribution in interval Θ_n.

Earlier, basing on the $Q_{2\alpha p}$ energy distribution of the triples $2\alpha + p$ from the "white" stars ^{10}C → $2\alpha + 2p$ it is concluded that in the ^{10}C nucleus the core ^{9}B is manifested with a probability of 30 ± 4 %, and the $^{8}Be_{g.s.}$ decays are arise always through the ^{9}B decays. An interesting feature is manifested in excitation energy distribution $Q_{2\alpha 2p}$ of $2\alpha 2p$ "quartets" provided by completeness of their observation. Fig. 13a shows distribution $Q_{2\alpha 2p}$ of all "white" stars ^{10}C → 2He + 2H which appears at a first glance to be scattered. The distribution $Q_{2\alpha 2p}$ of the ^{10}C stars containing ^{9}B decays features the distinct peak with a maximum at 4.1 ± 0.3 MeV at RMS of 2.0 MeV. Its width is determined by the accepted momentum approximation. The peak statistics present 17 ± 4 % of the total number of the ^{10}C "white" stars or 65 ± 14 % of those containing ^{9}B decays.
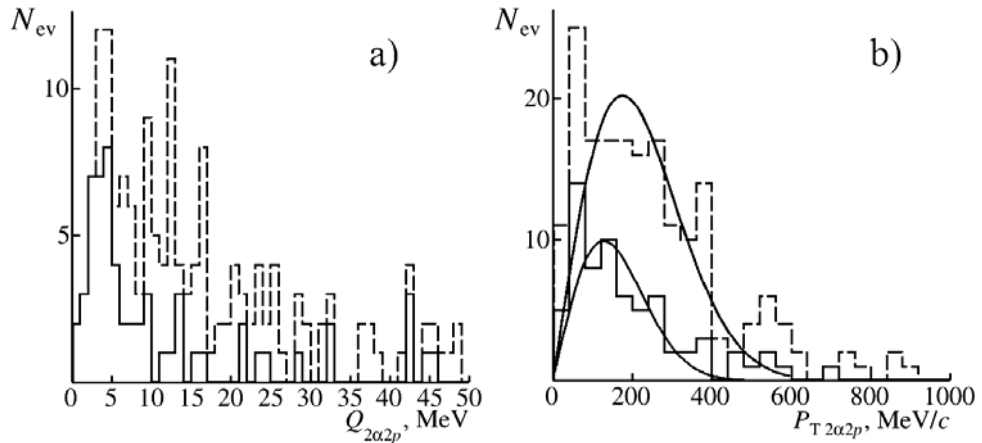

Fig. 13. Distributions over energy $Q_{2\alpha 2p}$ (a) and total transverse momentum $P_{T2\alpha 2p}$ (b) of all "white" stars ^{10}C → 2He + 2H (dashed) and the ones with the presence of ^{9}B (solid).

Distribution over a total momentum $P_{T2\alpha 2p}$ of all $2\alpha 2p$ ensembles (fig. 13b) is described by a Rayleigh function with the parameter $\sigma = 175 \pm 10$ MeV/c while in the case of the presence of $^{8}Be_{g.s.}$ (^{9}B) decays it is significantly less $\sigma = 127 \pm 16$ MeV/c. Not competing in statistics and resolution [4] our observation of such a state manifesting in extra narrow $2\alpha 2p$ jets is grounded on selection of evidently glancing collisions which reduce dramatically a continuum contribution. It is worth noting the observation of a single "white" star $2\alpha 2p$ having $Q_{2\alpha 2p}$ equal to 0.77 MeV in which both $2\alpha p$ triples correspond to ^{9}B decays with $Q_{2\alpha p}$ of 0.22 and 0.67 MeV, $Q_{2\alpha}$ of 0.14 MeV and $Q_{\alpha 2p}$ of 0.64 and 0.6 MeV (fig. 11).
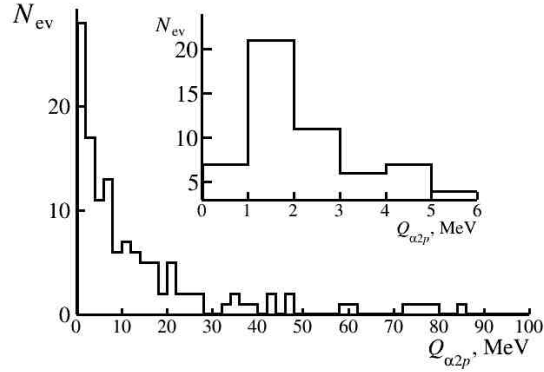
Fig. 14. Distributions over energy $Q_{\alpha 2p}$ in measured "white" stars ^{7}Be $\rightarrow$ He + 2H; on insertion: the enlarged $Q_{\alpha 2p}$ distribution in the ^{6}Be region.
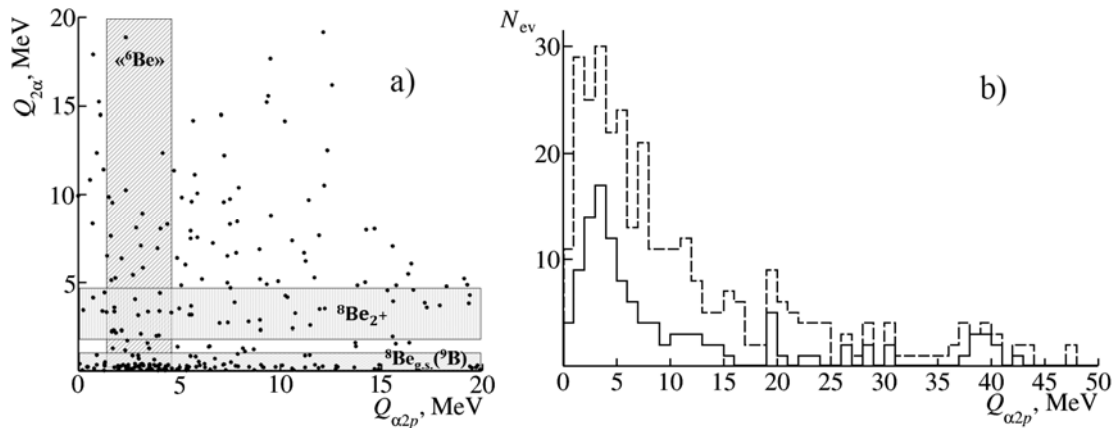

Fig. 15. Distributions of "white" stars ^{10}C $\rightarrow$ 2He + 2H over energy $Q_{2\alpha}$ and $Q_{\alpha 2p}$ (a, expected regions of decays ^{6}Be, ^{8}Be$_{g.s.}$ (^{9}B) and ^{8}Be$_{2+}$ are shown). Distributions of α2p triples over energy $Q_{\alpha 2p}$ in all "white" stars ^{10}C $\rightarrow$ 2He + 2H (b, dashed histogram) and with presence of ^{8}Be$_{g.s.}$ (^{9}B) decays in them (b, solid histogram).

High statistics of "white" stars He + 2H produced by 1.2 A GeV ^{7}Be nuclei [5] allows one to estimate the contribution of the unbound ^{6}Be nucleus in the distribution over $Q_{\alpha 2p}$ (fig. 14). 27 ± 5 % of 130 events in the channel He + 2H can be attributed to ^{6}Be decays by the condition $Q_{\alpha 2p}$ < 6 MeV. Contribution of the configuration ^{6}Be + n to the ^{7}Be structure is estimated at a level of 8 ± 1 % which is near fo the value of 5 ± 1 % for the configuration ^{6}Li + p. Detection efficiency of the last one is somewhat less. So, the difference of probabilities can be considered as unsignificant.

Determination of the ^{6}Be decay region gives an opportunity to estimate a possible ^{6}Be contribution to the ^{10}C "white" stars. Fig. 15a shows the correlation between $Q_{2\alpha}$ and $Q_{\alpha 2p}$. A peak at 3-4 MeV in the total distribution $Q_{\alpha 2p}$ covers totally the expected ^{6}Be signal. The peak is becoming profound when ^{8}Be$_{g.s.}$ decays in the stars are demanded (Fig. 15b). Surprisingly, but one can not separate the ^{6}Be and ^{8}Be$_{g.s.}$ decays and have to assume that ^{6}Be and ^{8}Be$_{g.s.}$ are produced as interfering parts of 2α2p ensembles.

Dissociation of the ^{11}C nucleus

The ^{11}C isotope combines peculiarities of stable nuclei with a pronounced α-particle clustering and nuclei at the boundary of proton stability where ^{3}He clustering is of the same importance. Interactions in the ensemble 2^{4}He + ^{3}He lead to the weakly bound configurations ^{7}Be + α (7.6 MeV), ^{10}B + p (8.7 MeV) and ^{3}He + ^{8}Be (9.2 MeV).

Exposure of a series of NTE samples is performed in the secondary beam of relativistic nuclei ^{11}C of the JINR Nuclotron. Nuclei ^{11}C were produced in fragmentation of nuclei ^{12}C of

13

energy 1.2 *A* GeV. Reduced thickness and glass substrates of an experimental batch of NTE are factors which do not allow carrying out an analysis with scanning along beam tracks without sampling. Therefore, scanning of the NTE layer was carried out on transverse strips. Tracks corresponding doubly and singly charged relativistic particles are determined visually. Dominance in the beam of C nuclei allows specifying charges of heavier fragments in "white" stars as values missing up to six charge units.

To date, 144 "white" stars with a total charge of relativistic fragments equal to 6 are found in scanned layers. Their distribution over charge states is presented jointly with comparable data on the isotopes ^{10}C and ^{9}C in Table 3. Table 3 demostrates the specific nature of "white" stars of each of the isotopes and compliance of the performed exposures to the mass numbers of the C isotopes. In the study of coherent dissociation of relativistic ^{12}C nuclei all found 100 "white" stars emerged in a single channel ^{12}C $\rightarrow$ 3He clearly reflecting the 3α-particle clustering of this nucleus. The key observation then became decays of unbound relativistic ^{8}Be nuclei which gave the contribution of not less than 20%.

Table 3. Distribution of "white" stars produced by the C isotopes at 1.2 *A* GeV over charge channels

Channel	^{11}C [12]	^{10}C [9]	^{9}C [5]
B + H	6 (4%)	1 (0.4 %)	15 (14 %)
Be + He	17 (12%)	6 (2.6 %)	
Be + 2H			16 (15 %)
3He	26 (18%)	12 (5.3 %)	16 (15 %)
2He + 2H	72 (50%)	186 (82 %)	24 (23 %)
He + 4H	15 (11%)	12 (5.3 %)	28 (27 %)
Li + He + H	5 (3%)		
Li + 3H		1 (0.4 %)	2 (2 %)

Events containing only the relativistic isotopes of He and H (77%), in particular, 2He + 2H dominate among the ^{11}C "white" stars. The ratio of this channel statistics to the statistics of the channel He + 4H is 5 ± 2. It does not correspond to only dissociation of the ^{7}Be core mentioned above. In contrast to the previously studied neutron deficient nuclei the significant share of events Li + He + H is observed, which could correspond to ^{6}Li + ^{4}He + *p*. There are no events Be + 2H which could correspond to ^{9}Be + 2*p*. However, there is a significant fraction of events Be + He in which the isotope ^{7}Be is uniquely determined. Most likely that the 3He channel corresponds to the configuration 2^{4}He^{3}He which can arise as from the break-ups of the core nuclei ^{8}Be and ^{7}Be and "dilute" 3He states. Additional contribution to the multiple He and H channels can be made cluster dissociation ^{6}Li, as a separate element of the ^{11}C according to the bond structure α + *d*. Figuratively being expressed the charge topology distributions have an individual character to ^{11}C which different from the other isotopes as a kind of "autograph".

Emission angles of fragments were measured in 156 dissociations ^{11}C $\rightarrow$ 2He + 2H among (212 found) including 62 "white" (72 found). The distributions over the opening angle Θ_{2He} of He fragments (Fig. 16, left) points to the presence of 16 decays ^{8}Be$_{g.s.}$ in "white" stars amouting them 24 ± 7 % in this channel. In the same way, 26 "white" stars of the 3He channel contain 7 decays ^{8}Be$_{g.s.}$ (fig. 17) amouting 27 ± 11 % in this channel and 5 ± 2 % of the channel ^{8}Be$_{g.s.}$ + ^{3}He in the overall statistics (Table 3). Besides, the distributions allow one to assume a strong contribution of ^{8}Be$_{2+}$ decays but it is a subject of future detailed consideration.

The virtual ^{9}B nucleus can exist in the ^{11}C nucleus as an independent component or as a component of a virtual core ^{10}B or ^{10}C. ^{9}B decays are identified by the small opening angle between directions of ^{8}Be$_{g.s.}$ and each one of H fragments $\Theta(^8$Be$_{g.s.}$ + H) < 25 mrad (Fig. 18). In the same way, 14 ^{9}B decays are identifyied in "white" stars ^{11}C $\rightarrow$ 2He + 2H (Fig. 18, left). Important conclusion is that being almost the same as the ^{8}Be$_{g.s}$ number the ^{9}B decay number

points on predominantly cascade production $^8Be_{g.s.}$ via ^9B like in the ^{10}C case. On this ground the channel $^9B + H$ amounts 14 ± 3 %. of the channel in the ^{11}C "white" star statistics (Table 3).

Preliminary, correspondence of H to p and He to α can be assumed in calculation $Q_{2\alpha 2p}$. Worth mentioning is the lowest energy peak in the distribution $Q_{2\alpha 2p}$ of 18 found stars $^{11}C \rightarrow$ 2He + 2H containing ^9B decays (fig. 19). In two cases both $2\alpha p$ triples correspond to ^9B decays. Having the same meaning as one in the ^{11}C case it is characterized by a somewhat less mean value of 2.7 ± 0.4 MeV at RMS of 2.0 MeV. A tendency can be noted that the ^9B condition selects "coldest" events among stars 2He + 2H.
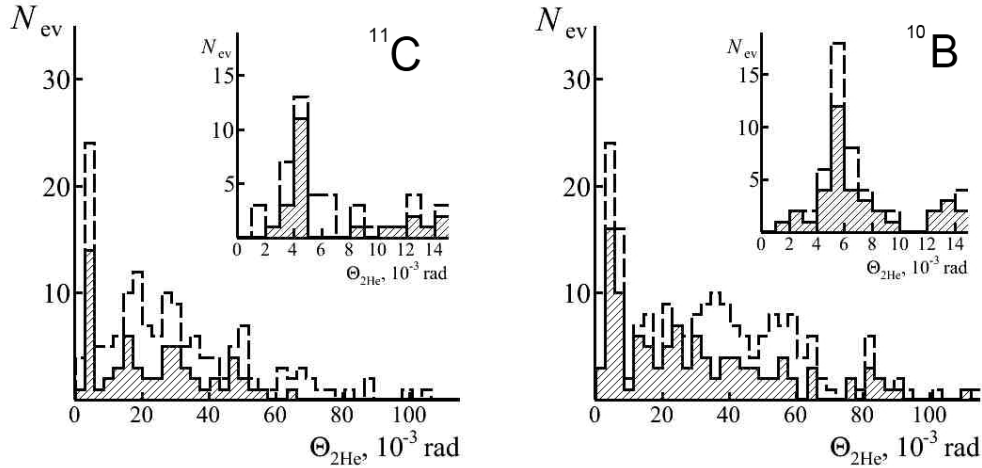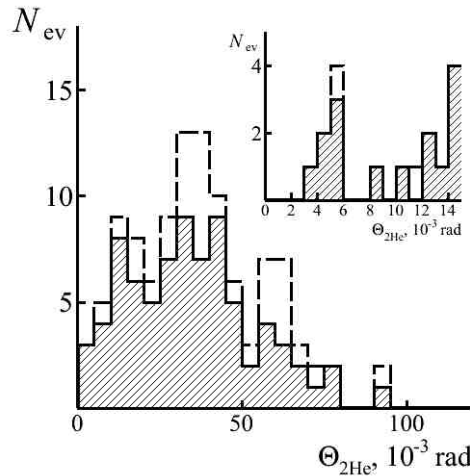

Fig. 16. Distributions over opening angle Θ_{He} between measured directions of He fragments in all ^{11}C stars 2He + 2H (a, dashed), "white" ^{11}C stars 2He + 2H (a, hatched), all ^{10}B stars 2He + H (b, dashed) and "white" ^{10}B stars 2He +H (b, hatched).

Fig. 17. Distributions over opening angle Θ_{He} between measured directions of He fragments in all ^{11}C stars 3He (a, dashed) and "white" ^{11}C stars 3He(a, hatched).
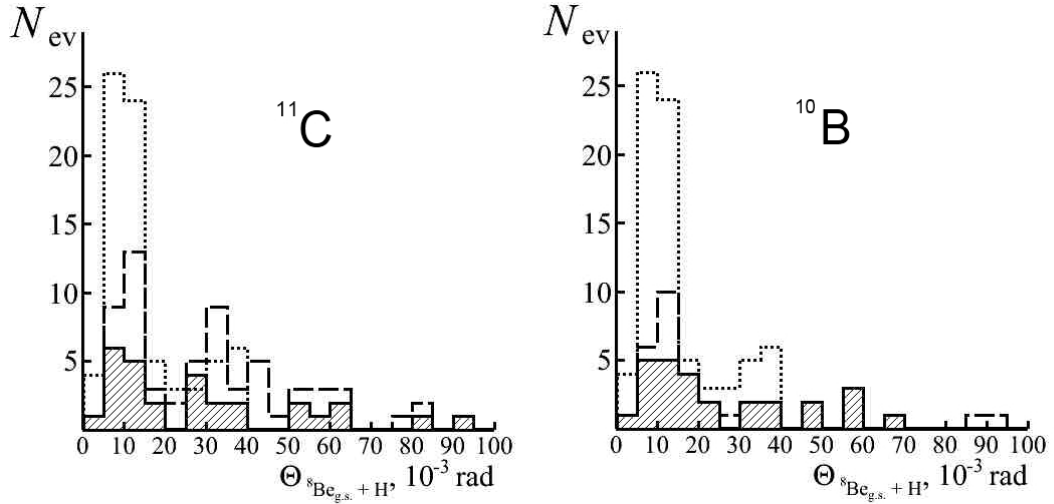
Fig. 18. Distributions over opening angle $\Theta_{8Be_{g.s.}+H}$ between measured directions of fragments $^{8}Be_{g.s.}$ and H fragments in ^{10}C "white" stars (dotted), all ^{11}C stars (left, dashed), "white" ^{11}C stars (left, hatched), all ^{10}B stars (right, dashed) and "white" ^{10}B stars (right, hatched).
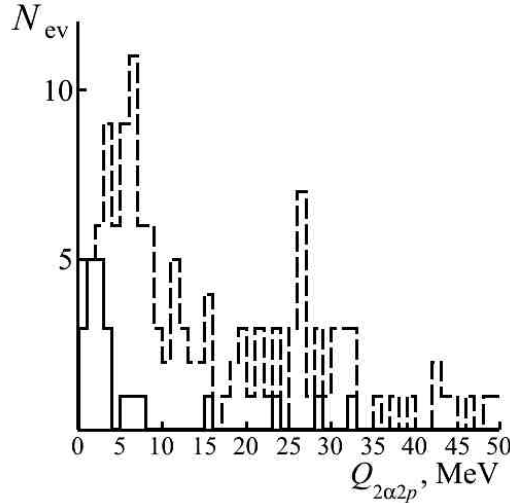

Fig. 19. Distributions over energy $Q_{2\alpha 2p}$ of all found stars $^{11}C \rightarrow 2He + 2H$ (dashed) and the ones with the presence of ^{9}B (solid).

Resumed analysis of dissociation of the ^{10}B nucleus

The early analysis of the NTE exposed in 2002 to 1 A GeV ^{10}B nuclei has pointed out that triples 2He + H constitute about 65% among 50 "white" stars found to that time. However, origins of this effect have not been studied being in a "shadow" of emerging studies with radioactive nuclei. Meanwhile, the the 2He + H triple dominance indicate the possible presence in ^{10}B of structures $^{9}B_{g.s.} + n$ side by side with the mirror one $^{9}Be + p$. It is interesting to verify whether they have equal contribuinity or not. Another opportuinity is that the ^{10}B nucleus can incorporate the "dilute" ^{9}Be cluster in the superpositions $^{8}Be_{g.s.} + n$ and $^{8}Be_{2+} + n$. Both them are leading to 3-prong "white" stars out of $^{9}B_{g.s.}$ decays. Thus, a new round of the ^{10}B analysis is started recently which progress is summarized below
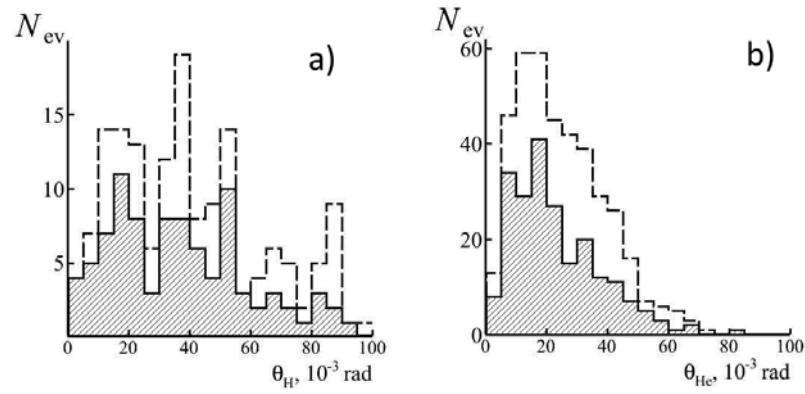
Fig. 20. Distributions for channel 2He + H over emission angles of fragments θ_{He} and θ_H in all found ^{10}B stars (a, dashed) and "white" ^{10}B stars (a, hatched).
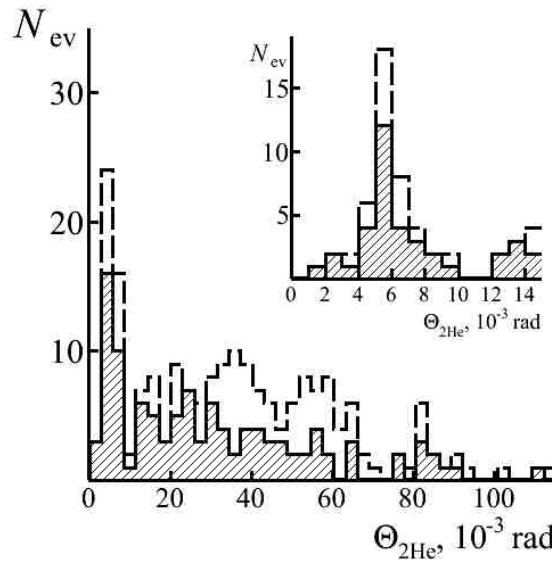

Fig. 21. Distributions over the opening angle Θ_{2He} of 2α pairs of all found (dashed) and "white" (hatched) stars ^{10}B → 2He + H.

A significant increasing statistics of stars ^{10}B → 2He + H is reached in an accelerated search for paired tracks when scanning is performed along transverse strips of NTE layers. Early, such an approach allowed one to obtain statistics of 500 events ^{9}B → 2He in a reasonable labour time. To date, measurements of emission angles of relativistic fragments are performed in 200 events ^{10}B → 2He + H including 108 "white" stars (fig. 20).

The distribution of 2He pairs over the opening angle Θ_{2He} in an interval $0 < \Theta_{n(arrow)} <$ 10.5 mrad allows one to count 54 decays ^{8}Be$_{g.s.}$ in all found events ^{10}B → 2He + H including 37 in the "white" stars (fig. 21). These numbers give 27 ± 4 % and 34 ± 7 % in the respective statistics. Then, the condition on the opening angle $\Theta(^8Be_{g.s.} + H) < 25$ mrad (fig. 16, right) allows one to identify 21 decays ^{9}B in all found events and 15 in the "white" stars which constitute, respectively, 11 ± 3 % and 14 ± 4 % contributions of the subset ^{8}Be$_{g.s.}$ + H in the channel 2He + H. Thus, the idea about of simultaneous presence in ^{10}B of superposition ^{8}Be$_{g.s.}$-^{8}Be$_{2+}$ and ^{9}B obtain a ground.
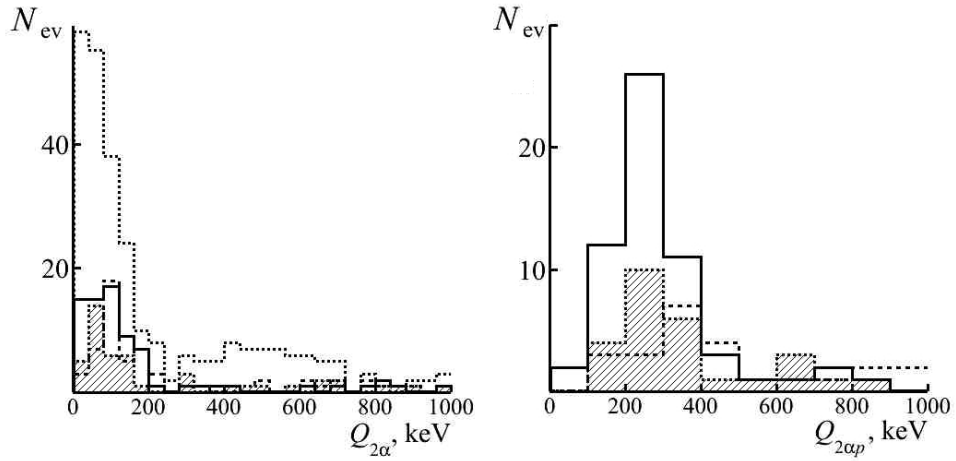
Fig. 22. Distributions of all found stars ^{9}Be → 2He (left top, dotted), ^{10}B → 2He + H, ^{11}C → 2He + 2H (hatched) and "white" stars ^{10}C → 2He + 2H (solid) over energy $Q_{2\alpha}$ of 2α pairs and energy $Q_{2\alpha p}$ of 2αp triples.

The distributions of the energy of α-particle pairs $Q_{2\alpha}$ and 2α + p triples $Q_{2\alpha p}$ from the foumd ^{10}B → 2He + H events shown in Fig. 22 arrange a common ensemble with the considered cases ^{9}Be, ^{10}C and ^{11}C. Correct positioning of the peaks ^{8}Be$_{g.s.}$ and ^{9}B can be noted. Thus, evolution of structural changes related with the unstable nuclei obtains an experimental extended ground.

Identification of He and H isotopes by a multiple scattering method progressing now will promote the analysis. In particular, the cluster configuration involving the deuteron ^{8}Be$_{2+}$ + d can be a source of ^{8}Be$_{2+}$ decays. Besides, since the channel ^{10}B → ^{6}Li + α is observed with 10% probability contribution of the "dilute" ^{6}Li cluster into the 2α + p(d) channel can be expected. Thus, with attraction of existing knowledge on ^{9}Be and ^{6}Li the pattern ^{10}B dissociation via decays ^{8}Be$_{g.s.}$, ^{8}Be$_{2+}$ and ^{9}B can be disentangled step by step. If successful, it will lead to better understanding for the neighbouring nuclei ^{11}C and, then, ^{12}N.

Summary
To conclude, the presented low and high energy exposures of NTE allowed one to perform a wide study of the role of the unstable nuclei to cluster degrees in light nuclear structures.

Nuclear track emulsion made it possible to identify decays of stopped ^{8}He nuclei, estimate possibilities of α-range spectrometry and observe the drift of thermalized ^{8}He atoms. The ^{8}He analysis can serve as a prototype for studying the decays of stopped radioactive nuclei.

Correlations of α-particles are studied on statistics of 400 events of splitting ^{12}C → 3α in nuclear track emulsion exposed to 14.1 MeV neutrons. Measurements of ranges and emission angles of the α-particles are performed. Distributions over energy of α-particle pairs and triples are obtained. In general, these data indicate the presence of a superposition of states 0^+ and 2^+ of the nucleus ^{8}Be in the ground state of ^{12}C.

In boron enriched NTE angular and energy correlations of products of the reaction induced by thermal neutrons n_{th} + ^{10}B → ^{7}Li + (γ) + α are studied. The distribution over the angle between reconstructed directions of emission of γ-quanta and nuclei ^{7}Li shows a clear anticorrelation and no correlation with α-particles. This fact demonstrates the production of the exited ^{7}Li nucleus.

Contribution of the unstable nuclei ^{6}Be, ^{8}Be and ^{9}B into dissociation of relativistic nuclei ^{7,9}Be, ^{10}B and ^{10,11}C is under study on the basis of NTE exposed to secondary beams of the JINR Nuclotron.

On the basis of angular measurements 27 ± 5 % of events ^{7}Be → He + 2H can be attributed to ^{6}Be decays. Contribution of the configuration ^{6}Be + n to the ^{7}Be structure is estimated at a level of 8 ± 1 % which is near the value of 5 ± 1 % for the configuration ^{6}Li + p.

Distributions over the opening angle of α-pairs indicate to a simultaneous presence of virtual ^{8}Be$_{g.s.}$ and ^{8}Be$_{2+}$ states in the ground states of the ^{9}Be and ^{10}C nuclei. The core ^{9}B is manifested in the ^{10}C nucleus with a probability of 30 ± 4 %. ^{8}Be$_{g.s.}$ decays in ^{10}C "white" stars always arise through the ^{9}B decays. For ^{10}C "white" stars it have to be assumed that ^{6}Be and ^{8}Be$_{g.s.}$ are produced as interfering parts of 2α2p ensembles due to impossibility of separation of the ^{6}Be and ^{8}Be$_{g.s.}$ decays. Selection of the ^{10}C "white" stars accompanied by ^{8}Be$_{g.s.}$ (^{9}B) leads to appearance in the excitation energy distribution of 2α2p "quartets" of the distinct peak with a maximum at 4.1 ± 0.3 MeV.

^{8}Be$_{g.s.}$ decays are presented in 24 ± 7 % of 2He + 2H and 27 ± 11 % of the 3He of the ^{11}C "white" stars. ^{9}B decays are identified in "white" stars ^{11}C → 2He + 2H constituting 14% of the ^{11}C "white" stars. As in the ^{10}C case ^{8}Be$_{g.s.}$ decays in ^{11}C "white" stars almost always arise through ^{9}B decays. On this ground the channel ^{9}B + H amounts 14 ± 3 %.

The ^{8}B$_{g.s.}$ nucleus is manifested in the "white" stars ^{10}B → 2He + H with a probability of 34 ± 7 % while ^{9}B constitute 14 ± 4 %. Thus, the decays ^{9}B account roughly for a half of the ^{8}Be$_{g.s.}$ statistics. This way, a ground appears to assume a additional contribution of virtual superposition ^{8}Be$_{g.s.}$-^{8}Be$_{2+}$ in the ^{10}B structure likewise the ^{9}Be case.

A good separation of carbon isotopes at the Nuclotron confirmed by data on their coherent dissociation indicates the possibility of exposure of NTE to isotopes ^{12,13}N produced in fragmentation of relativistic nuclei ^{14}N to increase dramatically the statistics of "white" stars. New opportunities could be opened when accelerating nuclei ^{16}O for such studies using beams of neutron-deficient isotopes ^{13,14,15}O. Further promotion by the NTE technique to heavier neutron-deficient isotopes keeps perspective, although it is getting harder. In this way it is possible to further increase diversity of studied ensembles of p-^{3}He-α.

It should be noted that for the nuclei ^{11}C and ^{12}N comes into play restriction of approach based on coherent dissociation of relativistic nuclei in NTE consisting in the inability of a direct identification of mass numbers of relativistic fragments heavier than He. Shares of events with participation of such fragments should increase rapidly with increasing mass number of a nucleus under study. This identification is possible in electronic experiments with magnetic analysis in a range of energy of a few GeV per nucleon of beam nuclei. Studies using the NTE technique will keep the value for orientation of electron experiments on coherent dissociation of relativistic neutron-deficient nuclei. In perspective, identification is possible at energy of nuclei in the region of tens of GeV per nucleon in experiments with hadron calorimeters.

References

1. The BECQUEREL Project WEB site: becquerel.jinr.ru.

2. C. F. Powell, P. H. Fowler, and D. H. Perkins, *Study of Elementary Particles by the Photographic Method* (Pergamon, London, 1959), pp. 465–472.

3. W. H. Barkas *Nuclear Research Emulsions*. New York – London: Academic Press, 1963.

4. Y. Goldschmidt-Cremont Photographic Emulsions. *Annu. Rev. Nucl. Sci.* 1953.

5. P. I. Zarubin "Tomography" of the cluster structure of light nuclei via relativistic dissociation" Lecture Notes in Physics **875**, Clusters in Nuclei, vol. 3, 51–93 (2014), Springer International Publishing (*and references herein*); *arXiv*: 1309.4881.

6. N. G. Peresadko *et al.* "Role of the Nuclear and Electromagnetic Interactions in the Coherent Dissociation of the Relativistic ^{7}Li Nucleus into the ^{3}H + ^{4}He Channel" Phys. At. Nucl. **88**, 75–79 (2008).

7. N. G. Peresadko *et al.* "Fragmentation of ^{7}Li Relativistic Nuclei on a Proton into the ^{3}H + ^{4}He Channel" Phys. At. Nucl. 73, 1942–1947 (2010).

8. N. K. Kornegrutsa *et al* "Clustering features of the ^{7}Be nucleus in relativistic fragmentation" Few Body Syst. **55** 1021–1023 (2014); arXiv: 1410.5162.

9. Yu. A. Aleksandrov *et al.* "Dissociation of Relativistic ^{7}Be Nuclei through the ^{3}He+^{4}He Channel on a Proton Target" Phys. At. Nucl. **78**, 363–368 (2015).

10. K. Z. Mamatkulov *et al.* "Dissociation of ^{10}C Nuclei in a Track Nuclear Emulsion at Energy of 1.2 GeV per Nucleon" Phys. At. Nucl. **76**, pp. 1224–1229 (2013); *arXiv*: 1309.4241.

11. R. R. Kattabekov *et al.* "Coherent Dissociation of Relativistic ^{12}N Nuclei" Phys. At. Nucl. **76**, 1219–1223 (2013); *arXiv*: 1310.2080.

12. D. A. Artemenkov *et al.* "Charge topology of coherent dissociation of ^{11}C and ^{12}N relativistic nuclei" Phys. At. Nucl. **78**, 794–799 (2015); arXiv: 1411.5806.

13. "Slavich Company JSC". WEB site: *www.slavich.ru, www.newslavich.com.*

14. D. A. Artemenkov *et al.* "Exposure of Nuclear Track Emulsion to ^{8}He Nuclei at the ACCULINNA Separator" Phys. Part. Nucl. Lett., **10**, 415–421(2013); *arXiv*: 1309.4808.

15. D. A. Artemenkov *et al.* "^{8}He nuclei stopped in nuclear track emulsion" Few-Body Systems **55**, 8-10, 733736 (2014); arXiv: 1410.5188.

16. P. I. Zarubin *et al.* "^{8}He nuclei stopped in nuclear track emulsion" Europe Physical Journal, Web of Conferences, 66, 11044, 2014;

17. R. R. Kattabekov *et al.* "Correlations of α-particles in splitting of ^{12}C nuclei by neutrons of energy of 14.1 MeV" Phys. At. Nucl. **76**, add. issue (Russian) 88–91(2013); *arXiv*: 1407.4575.

18. D. A. Artemenkov *et al.* "Irradiation of Nuclear Track Emulsions with Thermal Neutrons, Heavy Ions, and Muons" Phys. At. Nucl. **78**, 579–585 (2015); arXiv: 1407.572.

19. D. V. Kamanin, Y. V. Pyatkov "Clusterization in ternary fission" **875**, Clusters in Nuclei, vol. 3 184–246 (2013), Springer International Publishing (*and references herein*).

20. K. Z. Mamatkulov *et al.* "Toward an automated analysis of slow ions in nuclear track emulsion" Phys. Procedia **74,** 59–66 (2015); arXiv: 1508.2707.

21. F. Ajzenberg_Selove, Nucl. Phys. A **490**, 1–266 (1988); TUNL, Nuclear Data Evaluation Project. http://www.tunl.duke.edu/NuclData/

22. F. Ziegler, J. P. Biersack, and M. D. Ziegler, *SRIM — the Stopping and Range of Ions in Matter* (SRIM Co, 2008); Particle Interactions with Matter, SRIM –The Stopping and Range of Ions in Matter. http://srim.org/

23. V. M. Bystritsky *et al.* "DViN-2 Stationary Inspection Complex" Phys. Part. Nucl. Lett., **6**, 505–510 (2009).

24. "Image processing and analyses in Java". WEB site: http://rsb.info.nih.gov/ij/.